https://doi.org/10.52973/rcfcv-e363959 Revista Científica, FCV-LUZ / Vol. XXXVI

Ovine pulmonary adenocarcinoma associated with Jaagsiekte sheep retrovirus: Morphological, immunohistochemical and molecular findings

Adenocarcinoma pulmonar ovino asociado al retrovirus ovino de la Jaagsiekte: estudios morfológicos y moleculares

Canan Akdeniz - Incili[1], Yesari Eroksuz*[1], Mehmet Gül[2], Hasan Abaylı[3], Burak Karabulut[1], Hatice Eroksuz[1]

[1] Firat University, Faculty of Veterinary Medicine, Department of Pathology. 23 119,Elazig–Türkiye
[2] İnönü University, Faculty of Medicine, Department of Histology and Embryology. 44 280, Malatya-Türkiye
[3] Firat University, Faculty of Veterinary Medicine, Department of Virology. 23 119 Elazığ-Türkiye
**Corresponding author: yeroksuz@firat.edu.tr*

ABSTRACT

Ovine pulmonary adenocarcinoma is a contagious pulmonary neoplasm of sheep associated with exogenous Jaagsiekte sheep retrovirus. This retrospective descriptive case series characterized seven suspected ovine pulmonary adenocarcinoma cases using histopathology, immunohistochemistry, and semi-nested polymerase chain reaction on archived formalin-fixed, paraffin-embedded lung tissues. Fresh pulmonary tissue from two cases was also examined by transmission electron microscopy. Histopathological findings were compatible with ovine pulmonary adenocarcinoma in all cases and consisted of well-differentiated bronchioloalveolar epithelial proliferations arranged in papillary and acinar/tubular patterns. Cytoplasmic immunoreactivity for the jaagsiekte sheep retrovirus envelope protein was detected in neoplastic epithelial cells and in non-neoplastic type II pneumocytes. Immunolabelling was also observed in alveolar macrophages and lymphocytes in some cases; this finding was interpreted cautiously because it may reflect uptake of viral antigen rather than productive infection. Nuclear thyroid transcription factor-1 immunolabelling in neoplastic cells supported pulmonary epithelial differentiation. Semi-nested polymerase chain reaction provided molecular support by amplifying the expected 133 bp jaagsiekte sheep retrovirus -specific product in clearly positive samples, although band intensity varied among lanes. Transmission electron microscopy demonstrated lamellar body-like structures, cytoplasmic vacuolation, vesiculation, and membranous-lamellar degeneration in alveolar epithelial cells, but clearly identifiable viral particles were not demonstrated. Therefore, the findings should be interpreted as descriptive evidence supporting jaagsiekte sheep retrovirus -associated ovine pulmonary adenocarcinoma, rather than as proof of productive jaagsiekte sheep retrovirus infection or as a diagnostic-performance study. Larger prospective studies incorporating viral ribonucleic acid detection, sequencing, or direct virion demonstration are required.

Key words: Ovine pulmonary adenocarcinoma; Jaagsiekte sheep retrovirus; immunohistochemistry; semi-nested polymerase chain reaction; transmission electron microscopy.

RESUMEN

El adenocarcinoma pulmonar ovino es una neoplasia pulmonar contagiosa de las ovejas asociada al retrovirus ovino Jaagsiekte exógeno. En esta serie retrospectiva y descriptiva, se evaluaron siete casos sospechosos de adenocarcinoma pulmonar ovino mediante histopatología, inmunohistoquímica y reacción en cadena de la polimerasa semi-anidada en tejidos pulmonares archivados, fijados en formalina e incluidos en parafina. Además, tejidos pulmonares frescos de dos casos fueron examinados mediante microscopía electrónica de transmisión. Las lesiones histopatológicas fueron compatibles con adenocarcinoma pulmonar ovino en todos los casos y se caracterizaron por proliferaciones epiteliales bronquioloalveolares bien diferenciadas, dispuestas en patrones papilares y acinares/tubulares. Se detectó inmunorreactividad citoplasmática frente a la proteína de envoltura del retrovirus ovino Jaagsiekte exógeno en las células epiteliales neoplásicas y en neumocitos tipo II no neoplásicos. También se observó inmunomarcación en macrófagos alveolares y linfocitos en algunos casos; este hallazgo debe interpretarse con cautela, ya que puede reflejar captación secundaria del antígeno viral más que infección productiva. La inmunomarcación nuclear para factor de transcripción tiroidea 1en las células neoplásicas apoyó la diferenciación epitelial pulmonar. La reacción en cadena de la polimerasa semi-anidada aportó apoyo molecular mediante la amplificación del producto específico esperado de 133 pb para retrovirus ovino Jaagsiekte exógeno en muestras claramente positivas, aunque la intensidad de las bandas varió entre los carriles. La microscopía electrónica mostró cuerpos lamelares, vacuolización citoplasmática, vesiculación y degeneración membranosa-lamelar en células epiteliales alveolares, pero no se demostraron partículas virales claramente identificables. Por lo tanto, los hallazgos deben interpretarse como evidencia descriptiva compatible con adenocarcinoma pulmonar ovino asociada a retrovirus ovino Jaagsiekte exógeno, y no como confirmación de infección productiva ni como un estudio de rendimiento diagnóstico. Se requieren estudios prospectivos más amplios que incorporen detección de ácido ribonuclico viral, secuenciación o demostración directa de viriones.

Palabras clave: Adenocarcinoma pulmonar ovino; retrovirus ovino de la jaagsiekte; inmunohistoquímica; reacción en cadena de la polimerasa semi-anidada; microscopía electrónica de transmisión.

Recibido: 24/03/2026 Aceptado: 24/06/2026 Publicado: 16/07/2026

INTRODUCTION

Ovine pulmonary adenocarcinoma (OPA) is a contagious pulmonary epithelial neoplasm of sheep associated with exogenous Jaagsiekte sheep retrovirus (JSRV). The virus has tropism for differentiated pulmonary epithelial cells, particularly type II pneumocytes and bronchiolar club cells, which are the principal target cells in OPA. Because OPA develops slowly, follows a chronic course, and has a prolonged incubation period, diagnosis remains difficult under field conditions [1, 2, 3].

Practical serological tests are not available for routine diagnosis; therefore, postmortem evaluation still relies mainly on gross pathology, histopathology, immunohistochemistry (IHC), and polymerase chain reaction (PCR). Histopathology is essential for recognizing characteristic bronchioloalveolar epithelial proliferation, but its specificity may be reduced when chronic bronchopneumonia, fibrosis, atelectasis, or other proliferative lung lesions are present. In such cases, IHC and PCR provide important ancillary support by demonstrating viral antigen and viral nucleic acid, respectively, including in formalin-fixed, paraffin-embedded (FFPE) tissues [1, 3, 4].

Several studies have described the pathological, immunophenotypic, and molecular features of OPA; however, retrospective case series using archived diagnostic material remain useful because they reflect the type of specimens most commonly available in routine veterinary pathology. The combined evaluation of histopathological lesions, viral antigen localization, and viral nucleic acid detection can strengthen the etiologic interpretation, provided that the limitations of each method are clearly recognized [1, 2, 4]. The aim of the present study was to characterize seven suspected OPA cases by histopathology, IHC, and semi-nested PCR using archived FFPE lung tissues. Transmission electron microscopy was additionally performed in two cases to evaluate ultrastructural epithelial alterations and to search for viral particles.

MATERIALS AND METHODS

Study design and sample collection

This study was designed as a retrospective descriptive case series based on archived diagnostic material. No experimental infection or live-animal procedure was performed. Archived FFPE lung tissues were obtained from sheep (*Ovis aries*) suspected of having OPA. The study material consisted of 3- to 6-year-old Akkaraman sheep from the provinces of Elazığ, Tunceli, and Malatya. A total of seven lung samples were obtained from necropsy cases submitted to the Department of Pathology, Faculty of Veterinary Medicine, Fırat University (Elazığ, Türkiye). All tissues had been fixed in 10 % neutral buffered formalin for approximately 3–4 days (d) and routinely processed by standard paraffin-embedding methods.

The inclusion criteria were gross pathological findings suggestive of OPA, availability of well-preserved FFPE lung tissue, and accessible case records including age, breed, and clinical history. According to flock history, the disease pattern was characterized by sporadic respiratory distress and occasional deaths.

Histopathological examination

Sections 4–5 µm thick were prepared from FFPE tissue blocks using a Leica RM2125 RTS microtome (Leica, Germany) and stained with hematoxylin and eosin (H&E). The histopathological diagnosis of OPA was based on multicentric bronchioloalveolar epithelial proliferation forming papillary and/or acinar/tubular structures, expansion or filling of alveolar spaces, and extension of neoplastic epithelial cells into adjacent alveolar and interstitial tissues.

Immunohistochemical method

For the immunohistochemical detection of JSRV antigen and thyroid transcription factor-1 (TTF-1), 4–5 µm thick sections were mounted on adhesive slides. After deparaffinization and rehydration, heat-induced antigen retrieval was performed in citrate buffer (pH 6.0) in a microwave oven (Simbo 363, P.R.C.). Endogenous peroxidase activity was blocked with 3 % hydrogen peroxide. Sections were incubated overnight at 4 °C (Arçelik 5223 NHEY, Türkiye) with a rabbit polyclonal antibody against the JSRV envelope protein and with an antibody against TTF-1 (clone 8G7G3/1, monoclonal mouse. The anti-JSRV antibody has been used previously in ovine OPA investigations, and its staining pattern in the present material was evaluated together with

TABLE I

Primary antibodies, antigen retrieval conditions, chromogens, and control procedures used for immunohistochemistry

Primary antibody	Antibody data	Dilution	Antigen retrieval	Chromogen	Positive control	Negative control
JSRV envelope protein (JSRV-EP)	Rabbit polyclonal anti-JSRV antibody; kindly provided by Dr. Massimo Palmarini, Virus Research Centre, Glasgow	1:200	Citrate buffer, pH 6.0; heat-induced retrieval	DAB	Confirmed OPA/JSRV-positive ovine lung tissue	Primary antibody replaced with antibody diluent
TTF-1	Clone 8G7G3/1; monoclonal mouse; Zeta Corp., CA, USA	1:100	Citrate buffer, pH 6.0; heat-induced retrieval	AEC	Normal sheep lung	Primary antibody replaced with antibody diluent

TTF-1: thyroid transcription factor-1,DAB:3,3′-diaminobenzidine; AEC:3-amino-9-ethylcarbazole; JSRV-EP: Jaagsiekte sheep retrovirus envelope protein.

negative controls and lesion distribution [5, 6, 7, 8]).

After washing, the sections were incubated with a polyvalent secondary antibody at 37 °C for 60 min. Immunoreactivity was demonstrated using the avidin-biotin complex streptavidin-peroxidase method with 3-amino-9-ethylcarbazole (AEC) as the chromogen for TTF-1 and 3,3′-diaminobenzidine (DAB) as the chromogen. Details of the primary antibodies, antigen retrieval conditions, chromogens, and control tissues used for immunohistochemistry are summarized in TABLE I. The slides were counterstained with Mayer's hematoxylin. Negative controls were prepared by replacing the primary antibody with antibody diluent.

Transmission electron microscopy

For transmission electron microscopy (TEM) evaluation, fresh pulmonary samples from tumor-containing regions of two cases were fixed in 3 % glutaraldehyde buffered with 0.2 M Sodium dihydrogen phosphate / Disodium hydrogen phosphate (NaH_2PO_4/Na_2HPO_4) (pH 7.2–7.3), post-fixed in 2 % osmium tetroxide (OsO_4), and embedded in Araldite CY 212. Ultrathin sections were stained with uranyl acetate and lead citrate and examined using a Zeiss Libra 120 transmission electron microscope (Carl Zeiss NTS GmbH, Oberkochen, Germany).

Deoxyribonucleic acid extraction and semi-nested polymerase chain reaction

Genomic deoxyribonucleic acid (DNA) was extracted from OPA-suspected lung tissues using a modified phenol-chloroform method [9]. Briefly, tissues were digested with proteinase K, followed by organic extraction, ethanol precipitation, and resuspension of the DNA pellet in nuclease-free water. DNA concentration and purity were evaluated spectrophotometrically (Thermo Fisher, MA, USA), and extracts were stored at −20 °C (Arçelik, Türkiye) until analysis. Detection of exogenous JSRV was performed by semi-nested PCR using a GeneAmp 9700 thermal cycler (Thermo Fisher, MA, USA), based on a previously described protocol with minor modifications [10]. Amplified products were visualized by electrophoresis on a 1.5 % agarose gel (Thermo Fisher, MA, USA). PCR results were interpreted according to the presence of a reproducible band of the expected size, together with positive and negative control reactions.

Data analysis

Because this study was designed as a retrospective descriptive case series, no inferential statistical analysis was performed. The findings were analyzed descriptively. Gross, histopathological, immunohistochemical, molecular, and ultrastructural findings were evaluated case by case and then summarized according to their frequency, distribution, staining pattern, PCR positivity, and concordance with the morphological diagnosis of ovine pulmonary adenocarcinoma. Immunohistochemical results were interpreted qualitatively based on the localization, intensity, and cellular distribution of immunolabelling. PCR results were interpreted according to the presence or absence of the expected 133 bp amplicon. Transmission electron microscopy findings were assessed descriptively for epithelial ultrastructural alterations and the presence or absence of identifiable viral particles.

RESULTS AND DISCUSSION

Gross pathology

At necropsy, all lungs (7/7) were markedly enlarged, heavy, and firm, with a meaty consistency. Grossly, the lesions were characterized by multifocal to coalescing cranioventral consolidations containing pale gray-white neoplastic foci in the apical, medial, or diaphragmatic lobes (FIG. 1A). On cut surfaces, multifocal to extensive gray-white, solid, raised, and firm areas of consolidation were observed in the affected parenchyma (FIG. 1B). Foamy fluid was present in the lumen of the trachea, bronchi, and bronchioles. In one case, hydrothorax was observed, with accumulation of approximately 500 mL of clear, non-clotting fluid in the thoracic cavity.

Histopathology

Microscopically, the pulmonary parenchyma was expanded by a well-differentiated, multicentric bronchioloalveolar epithelial neoplasm characterized by proliferation of cuboidal to columnar epithelial cells lining, expanding, and frequently filling alveolar spaces and bronchiolar lumina (FIG. 1C). The neoplastic cells were arranged in papillary and acinar/tubular patterns, and papillary projections were supported by delicate fibrovascular cores (FIG. 1C).

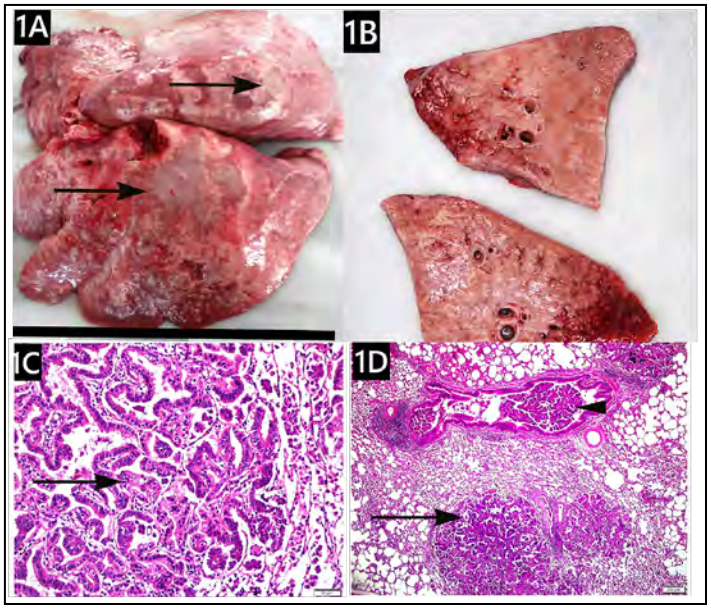

FIGURE 1. Gross and histopathological findings in the lungs of ovine pulmonary adenocarcinoma. 1A. Lung lobes showing multifocal to coalescing, gray-white, slightly raised neoplastic foci on the pleural surface (arrows). 1B. Cut surfaces of the lung showing well-demarcated, pale gray-white nodular areas within the parenchyma. 1C. Neoplastic tissue consists of papillary and acinar proliferations of epithelial cells supported by delicate fibrovascular stroma (arrow). H&E. Bar = 50 µm. 1D. Intraluminal bronchiolar papillary neoplastic proliferation (arrowhead) and a neoplastic focus in the adjacent pulmonary parenchyma (arrow). H&E. Bar = 200 µm

Multifocal neoplastic nodules were scattered throughout the pulmonary parenchyma, and intraluminal papillary growth occasionally extended into bronchiolar lumina (FIG. 1D). Adjacent areas showed alveolar atelectasis, variable fibrosis, and mild to moderate lymphohistiocytic infiltrates. Overall, the histomorphological features were consistent with well-differentiated bronchioloalveolar carcinoma (FIGS. 1C–D). In the case with chylothorax, both solitary and clustered metastatic foci were detected in the mediastinal lymph nodes. In another case, multifocal pulmonary abscesses were present. No myxoid growth was identified in any case.

Viral antigen detection and immunophenotype

Immunohistochemical examination showed strong intracytoplasmic immunoreactivity in multifocal to coalescing neoplastic proliferations (FIG. 2A). At higher magnification, diffuse cytoplasmic positivity was present in neoplastic bronchioloalveolar epithelial cells arranged in papillary and acinar structures; this pattern was consistent with JSRV antigen localization within the tumor epithelium (FIG. 2B). Cytoplasmic immunoreactivity was also detected in alveolar macrophages and lymphocytes in some cases (FIG. 2C). TTF-1 immunostaining showed marked nuclear immunoreactivity in neoplastic epithelial cells (FIG. 2D).

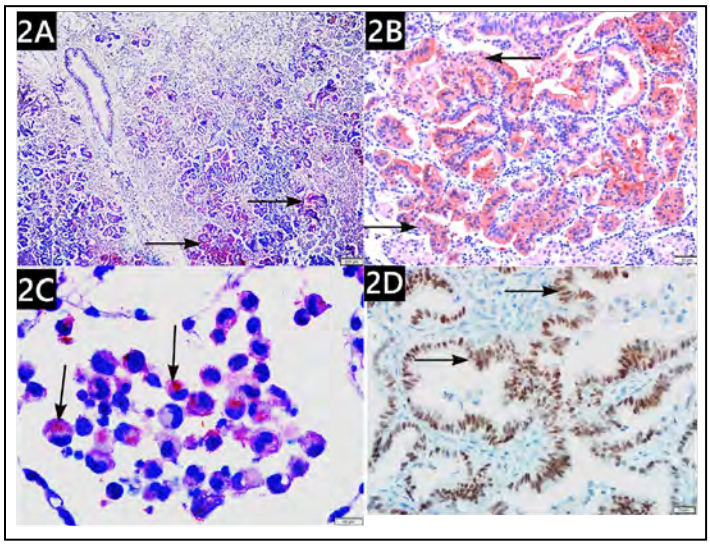

FIGURE 2. Immunohistochemical features of ovine pulmonary adenocarcinoma in the lung. 2A. Low-magnification immunohistochemistry image showing multifocal to coalescing neoplastic proliferations within the pulmonary parenchyma and strong intracytoplasmic immunoreactivity in tumor cells (arrows). Bar = 200 µm. 2B. Diffuse cytoplasmic immunoreactivity in neoplastic bronchioloalveolar epithelial cells arranged in papillary and acinar patterns, consistent with JSRV antigen localization (arrows). Bar = 50 µm. 2C. Alveolar macrophages showing positive cytoplasmic immunoreactivity (arrows). Bar = 10 µm. 2D. TTF-1 immunohistochemistry showing nuclear immunolabeling in neoplastic bronchioloalveolar epithelial cells (arrows), supporting pulmonary epithelial differentiation. Bar = 20 µm

Ultrastructural pathology

Transmission electron microscopic examination revealed prominent ultrastructural abnormalities in alveolar epithelial cells, particularly in cells morphologically compatible with type II pneumocytes (FIGS. 3A–D).

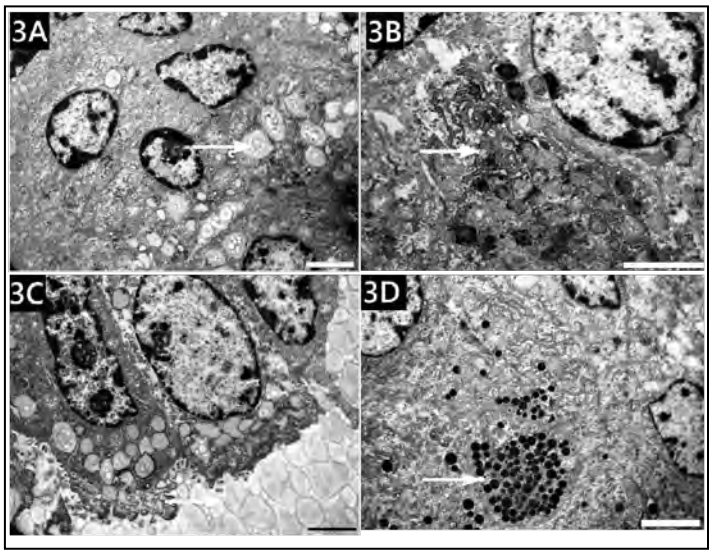

FIGURE 3. Transmission electron micrographs of lung tissue showing ultrastructural changes in alveolar epithelial cells, especially in cells morphologically consistent with type II pneumocytes in ovine pulmonary adenocarcinoma. 3A. Numerous membrane-bound vacuolar and vesicular structures are present in the cytoplasm; the arrow indicates an organelle with concentrically arranged membranous profiles consistent with a lamellar body. 3B. The arrow indicates irregular membranous-lamellar material and myelin figure-like structures within the cytoplasm. 3C. The arrow indicates an apical exocytotic profile consistent with release of secretory material into the alveolar lumen. 3D. Clusters of electron-dense granular structures within the cytoplasm (arrow)

Numerous membrane-bound vacuolar and vesicular structures of varying sizes were present in the cytoplasm (FIGS. 3A, C). Organelles containing concentrically arranged membranous profiles and consistent with lamellar bodies were also identified (arrow, FIG. 3A).

In addition, irregular membranous-lamellar material and myelin figure-like structures were observed in the cytoplasm (arrow, FIG. 3B), suggesting degenerative membrane remodeling. Exocytotic release features compatible with secretion of material into the alveolar lumen were prominent in the apical cytoplasm and along the luminal surface (FIG. 3C). Clusters of electron-dense granular material were also present within the cytoplasm (FIG. 3D). Overall, these ultrastructural findings support marked alterations in surfactant-related organelles and degenerative cytoplasmic changes in alveolar epithelial cells.

Semi-nested polymerase chain reaction findings

Following semi-nested PCR amplification, a product of the expected size (133 bp) was detected in clearly positive sample lanes and in the positive control, whereas other sample lanes were absent or only faintly detectable (FIG. 4). Because band intensity varied among the examined lanes, the PCR findings were interpreted as molecular support for JSRV-associated OPA rather than as stand-alone confirmation in every examined tissue.

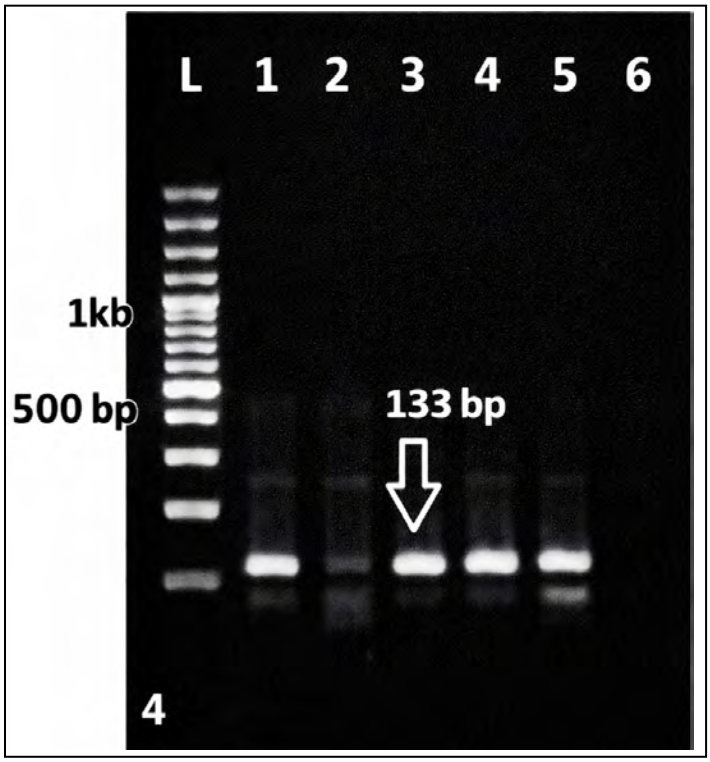

FIGURE 4. Agarose gel electrophoresis of PCR products. L: DNA ladder (1 kb and 500 bp markers). Lane 1: Positive control, Lane 2-5: Clinical samples, Lane 6: Negative control

The present study should be interpreted as a retrospective descriptive case series, not as an assessment of prevalence, diagnostic sensitivity, specificity, or marker performance. Within this scope, histopathology, IHC, and semi-nested PCR provided complementary evidence supporting JSRV-associated OPA in the examined diagnostic material [1, 4, 5, 10, 11, 12, 13]. This distinction is important because the study included only seven cases and used archived FFPE tissues, which may limit molecular yield and ultrastructural preservation.

The gross and histological lesions were compatible with the classical pathological spectrum of OPA. The main diagnostic features were multicentric bronchioloalveolar epithelial proliferation, papillary and acinar/tubular growth, expansion of alveolar spaces, and variable adjacent atelectasis, fibrosis, and lymphohistiocytic inflammation [1, 5, 13]. These findings reinforce the value of conventional histopathology as the diagnostic foundation, especially when it is supported by targeted IHC and PCR. Chronic suppurative bronchopneumonia, verminous pneumonia, fibrosis, and atelectasis should remain in the differential diagnosis because these lesions can mimic or obscure OPA in field cases [3, 8, 14].

The absence of myxoid growths in this series should be reported explicitly because myxoid or mesenchymal proliferations have been described in a subset of OPA cases. Toma et al. documented both classical and atypical forms of OPA and reported myxoid growths in a proportion of tumors, with a mesenchymal immunophenotype [8]. In the present material, the lesions were dominated by epithelial bronchioloalveolar proliferation, and no myxoid component was detected.

The immunohistochemical distribution of JSRV antigen was biologically consistent with the epithelial tropism of JSRV. Strong cytoplasmic immunoreactivity in neoplastic epithelial cells and non-neoplastic type II pneumocytes supports the association between the observed tumor phenotype and JSRV-related antigenic markers [5, 6, 7]. In contrast, immunolabelling in alveolar macrophages and lymphocytes should be interpreted with caution. Such staining may reflect phagocytosis, antigen uptake, or secondary exposure to viral material rather than productive infection of these cells [7, 13].

Thyroid transcription factor-1 nuclear immunolabelling supported pulmonary epithelial differentiation of the neoplastic cells. This interpretation is consistent with the study of Toma et al., who reported strong TTF-1 expression in the neoplastic epithelial component of classical and atypical OPA, whereas associated myxoid growths were TTF-1 negative and showed a mesenchymal phenotype [15]. However, TTF-1 positivity in the present small series should not be presented as validation of marker performance. It is best interpreted as supportive immunophenotypic evidence when used together with morphology and JSRV-directed testing.

The semi-nested PCR results added etiologic support but should not be overinterpreted. Detection of the expected 133 bp amplicon in clearly positive lanes supports the presence of JSRV-related nucleic acid in affected tissue. However, faint or absent bands in other lanes may reflect low template quantity, FFPE-associated DNA fragmentation, uneven distribution of infected or neoplastic cells, or technical variation. For this reason, the PCR data are most appropriately integrated with histopathology and IHC rather than presented as definitive confirmation in every case.

The TEM findings were supportive at the cellular level but not confirmatory for viral infection. Lamellar body-like structures, vesiculation, cytoplasmic vacuolation, and membranous-lamellar degeneration are compatible with marked alteration of type II pneumocyte surfactant-related organelles. Because definitive viral particles were not demonstrated, TEM should be described as showing epithelial injury and secretory-organelle remodeling, not direct virion visualization. This moderated interpretation directly reflects the limitation of the ultrastructural findings.

Ovine pulmonary adenocarcinoma has comparative relevance because it represents a spontaneous large-animal model of pulmonary epithelial tumorigenesis and viral oncogenesis. However, the translational value of this model depends on precise pathological interpretation and cautious integration of ancillary results [2, 11]. In routine diagnostic settings, especially when only archived FFPE material is available, the most defensible approach is to combine lesion morphology with JSRV antigen localization and molecular detection, while clearly stating the limitations of each method.

The main limitations of this study are the small number of cases, retrospective design, use of archived FFPE tissue for molecular testing, limited availability of fresh tissue for TEM, and absence of viral RNA detection, sequencing, or in situ hybridization. These limitations prevent conclusions about prevalence, assay performance, viral load, or productive infection. Future prospective studies should include larger case numbers, standardized sampling of tumor and non-tumor lung, viral RNA-based assays, sequencing, and, where possible, direct ultrastructural demonstration of virions.

CONCLUSION

In conclusion, this retrospective descriptive case series shows that the combined use of histopathology, IHC, and semi-nested PCR provides complementary evidence supporting JSRV-associated OPA in archived ovine lung tissues. The findings should not be interpreted as a diagnostic-performance assessment because only seven cases were examined. JSRV antigen localization in neoplastic epithelial cells and TTF-1 nuclear immunolabelling support pulmonary epithelial differentiation and JSRV association.

PCR detection of the expected 133 bp product provides additional molecular support, but variable band intensity requires cautious interpretation. TEM demonstrated marked epithelial injury and surfactant-related organelle remodeling; however, identifiable viral particles were not demonstrated. Larger prospective studies using viral RNA detection, sequencing, and direct virion demonstration are needed to confirm productive infection and to define the diagnostic contribution of each ancillary method.

Conflicts of interest

The authors declare that they have no competing interests related to the authorship or publication of this article.

Financial support

This research was conducted without external financial support.

BIBLIOGRAPHIC REFERENCES

[1] Griffiths DJ, Martineau HM, Cousens C. Pathology and pathogenesis of ovine pulmonary adenocarcinoma. J. Comp. Pathol. [Internet]. 2010; 142(4):260-283. doi: https://doi.org/djzksg

[2] Leroux C, Girard N, Cottin V, Greenland T, Mornex JF, Archer F. Jaagsiekte sheep retrovirus (JSRV): from virus to lung cancer in sheep. Vet. Res. [Internet]. 2007; 38(2):211-228. doi: https://doi.org/dgrbm7

[3] Quintas H, Pires I, Garcês A, Prada J, Silva F, Alegria N. The diagnostic challenges of ovine pulmonary adenocarcinoma. Ruminants. [Internet]. 2021; 1(1):58-71. doi: https://doi.org/rfcn

[4] Lewis FI, Brülisauer F, Cousens C, McKendrick IJ, Gunn GJ. Diagnostic accuracy of PCR for Jaagsiekte sheep retrovirus using field data from 125 Scottish sheep flocks. Vet. J. [Internet]. 2011; 187(1):104-108. doi: https://doi.org/djn6mp

[5] Beytut E, Sözmen M, Ergínsoy S. Immunohistochemical detection of pulmonary surfactant proteins and retroviral antigens in the lungs of sheep with pulmonary adenomatosis. J. Comp. Pathol. [Internet]. 2009; 140(1):43-53. doi: https://doi.org/fh96w7

[6] Platt JA, Kraipowich N, Villafane F, DeMartini JC. Alveolar type II cells expressing Jaagsiekte sheep retrovirus capsid protein and surfactant proteins are the predominant neoplastic cell type in ovine pulmonary adenocarcinoma. Vet. Pathol. [Internet]. 2002; 39(3):341-352. doi: https://doi.org/df5jww

[7] Martineau HM, Cousens C, Imlach S, Dagleish MP, Griffiths DJ. Jaagsiekte sheep retrovirus infects multiple cell types in the ovine lung. J. Virol. [Internet]. 2011; 85(7):3341-3355. doi: https://doi.org/dw82ph

[8] Toma C, Bâlteanu VA, Tripon S, Trifa A, Rema A, Amorim I, Pop RM, Popa R, Catoi C, Taulescu M. Exogenous Jaagsiekte Sheep Retrovirus type 2 (exJSRV2) related to ovine pulmonary adenocarcinoma (OPA) in Romania: prevalence, anatomical forms, pathological description, immunophenotyping and virus identification. BMC Vet. Res. [Internet]. 2020; 16:296. doi: https://doi.org/rfcp

[9] Can-Sahna K, Eroksuz Y, Berber E, Sozdutmaz I. Detection of exogenous Jaagsiekte sheep retrovirus in Turkey. Indian J. Anim. Res. [Internet]. 2015; 49(4):498-502. doi: https://doi.org/rfcq

[10] Rosato G, Abril C, Hilbe M, Seehusen F. A combined approach for detection of ovine small ruminant retrovirus co-infections. Viruses. [Internet]. 2023; 15(2):376. doi: https://doi.org/rfcr

[11] Coşkun N, Yılmaz V, Karakurt E, Beytut E, Nuhoglu H, Timurkan MO. Molecular and pathological detection of Jaagsiekte sheep retrovirus in lung tissues of sheep. Kafkas Univ. Vet. Fak. Derg. [Internet]. 2024; 30(6):809-814. doi: https://doi.org/rfcs

[12] Oda SS, Youssef SA. Immunohistochemical and histopathological findings of ovine pulmonary adenocarcinoma (Jaagsiekte) in Egyptian sheep. Trop. Anim. Health Prod. [Internet]. 2011; 43(8):1611-1615. doi: https://doi.org/frhbwb

[13] De las Heras M, González L, Sharp JM. Pathology of ovine pulmonary adenocarcinoma. Fan, H. (eds). Jaagsiekte Sheep Retrovirus and Lung Cancer. Curr. Top. Microbiol. Immunol. [Internet]. Berlin, Heidelberg, Germany: Springer. 2003; 275:25-54. doi: https://doi.org/cq6v5f

[14] Lee AM, Wolfe A, Cassidy JP, Messam LLMV, Moriarty JP, O'Neill R, Fahy C, Connaghan E, Cousens C, Dagleish MP, McElroy MC. First confirmation by PCR of Jaagsiekte sheep retrovirus in Ireland and prevalence of ovine pulmonary adenocarcinoma in adult sheep at slaughter. Ir. Vet. J. [Internet]. 2017; 70:33. doi: https://doi.org/gcrr5m

[15] Gray ME, Meehan J, Sullivan P, Marland JRK, Greenhalgh SN, Gregson R, Clutton RE, Ward C, Cousens C, Griffiths DJ, Murray A, Argyle D. Ovine pulmonary adenocarcinoma: A unique model to improve lung cancer research. Front. Oncol. [Internet]. 2019; 9:335. doi: https://doi.org/rfcv